Vibrational shifts of absorption bands of linear molecules diluted in high-density rare gases: Measurements and modeling for CO2-Rg and OCS-Rg

L. Troitsyna, R. Asfin, N. Gennadiev, J. Buldyreva, N. Filippov

Version of Record: https://www.sciencedirect.com/science/article/pii/S002240732030073X
Manuscript_911bf095196a3e98aea650f0ab0a91d4

Vibrational shifts of absorption bands of linear molecules diluted in high-density rare gases: Measurements and modeling for CO_2-Rg and OCS-Rg

L. Troitsyna[a,*], R. Asfin[b], N. Gennadiev[b], J. Buldyreva[a], N. Filippov[b]

[a] *Institut UTINAM UMR CNRS 6213, Université Bourgogne Franche-Comté, 16 route de Gray, Besançon 25030 cedex, France*
[b] *St Petersburg State University, 7/9 Universitetskaya emb., St Petersburg 199034, Russia*

Abstract

Increase of buffer gas pressure causes redistribution of intensity in the IR absorption bands and, indicating the presence of vibrational perturbation, changes the first spectral moment value responsible for the band-origin position. Band-origin shift coefficients for the ν_3, $2\nu_3$ and ν_2 bands of OCS and the ν_3 band of CO_2 diluted in high-density Ar, Kr and Xe are measured and calculated by two methods: directly with available in the literature vibrationally dependent potential-energy surfaces for both initial and final vibrational states and assuming that vibrational dependence arises from the interaction of the permanent /transient dipole moment of the absorbing molecule and the dipole moment induced on the perturber. A comparative analysis of results is given, showing a general underestimation of calculations with respect to measurements.

Keywords: Infrared absorption spectra, Band-origin shift, Spectral moments, Vibrational dependence, DID model, Carbon dioxide, Carbonyl sulfide, Rare gases

1. Introduction

Though molecular spectra contain information on the nature of intermolecular interactions and features of molecular structure, their interpretation is associated with numerous difficulties [1] still to be resolved. For instance, spectral band shapes change significantly with increasing pressure and a set of characteristics is required for description of the band under various experimental conditions. In particular, the spectral moments M_n account for numerous band properties and thus can be used for practical purposes, though even a complete set of spectral moments does not characterize a unique band. For examining the interaction mechanisms that result in specific-band properties, particularly suitable candidates are benchmark systems composed of linear molecules, such as CO_2 and OCS, perturbed by rare gases.

*Corresponding author larisa.troitsyna@univ-fcomte.fr

These two molecules are present in planetary atmospheres (94.9% and 96.5% of CO_2 for Mars [2] and Venus [3], respectively, and trace-gas level [4, 5] of OCS), comets [6, 7], and interstellar space [8, 9]. Precise knowledge of their spectral band shapes and band origins is therefore essential for reliable radiative transfer simulations and remote sensing of atmospheric environments. Line positions, intensities, widths and shifts have been closely considered in numerous works. For OCS-Ar e.g., line widths in the ν_1 [10] and hot [11] bands, line widths and shifts in the $2\nu_3$ band [12] have been measured. For CO_2-Ar, line shifts in the 00^03-00^00 band [13], line shifts, speed-dependence parameters and line mixing coefficients in the 30013-00001 and 30012-00001 bands [14] have been reported. In contrast, studies of band-origin shifts remain very scarce up to now due to two major reasons.

From the experimental standpoint, determination of the band-origin shift (defined by M_1 — see Sec. 3.2) requires accurate intensity measurements up to very far spectral wings, which is a tedious and time-consuming task because of the numerous neighboring bands to be removed. That is why, traditionally, the band-origin shift is rather estimated from the position of the intensity maximum, as it was done in the work of Ozanne *et al.* [15] who investigated the ν_3 and $3\nu_3$ bands of CO_2-Ar at pressures up to 1000 bar. The band shifts were determined as a deviation of the measured intensity maximum from its position computed by the Energy-Corrected Sudden model. The shifting coefficients were found to be $\gamma(\nu_3) = (-5.4\pm1.0)\times10^{-3}$ cm^{-1} amagat^{-1} and $\gamma(3\nu_3) = (-17.0\pm1.0)\times10^{-3}$ cm^{-1} amagat^{-1}.

From the theoretical viewpoint, accurate band-origin shift calculations require vibrationally dependent potential energy surfaces (PESs) for both initial (ground) and final (excited) states, that are currently available only for a limited amount of systems. If the vibrational dependence of the final-state PES is unknown, mechanisms responsible for inducing the band-origin shift must be examined (e.g., Ozanne and coauthors [15] suggested that the polarizability matrix elements of a linear molecule are vibrationally dependent).

In the present work we perform accurate high-pressure measurements of CO_2-Rg (up to 100 atm) and OCS-Rg (up to 300 atm) band shapes and rigorously compute the band-origin positions from the first moment definition (see Sec. 4.1). Moreover, we suggest that, in the absence of vibrationally-dependent PES, the interaction between the dipole moment induced on the atom and the dipole of the molecule (DID interaction) can also result in a band-origin shift and test this hypothesis by comparing the results of the DID model and those obtained with vibrationally-dependent PES for both initial and final states. In Section 2 we briefly describe the experimental conditions. Theoretical background is summarized in Section 3. Details of modeling for CO_2 and OCS are given in Sec. 3.2. The bulk of our experimental and theoretical results is discussed and compared with that of Ref. [15] in the final section.

2. Measurements

IR absorption spectra of CO_2-Ar, CO_2-Kr, CO_2-Xe, OCS-Ar and OCS-Kr gas mixtures at 298 K were registered with Bruker IFS-28 and Bruker IFS 125/HR spectrometers in the region 400–4500 cm^{-1} with a spectral resolution 0.8 cm^{-1}. Active-gas concentrations were at trace-gas level, and the buffer-gas pressures varied from 15 to 100 atm for CO_2-Rg and from 25 to 300 atm for OCS-Rg. In function of the studied spectral range and the mixture

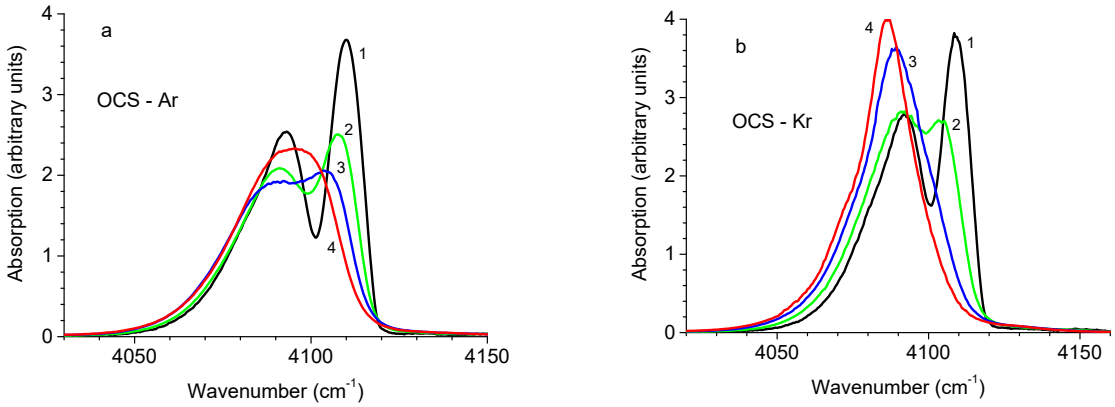

Figure 1: $2\nu_3$ OCS-Ar (a) and OCS-Kr (b) band shapes at buffer-gas pressures of 25 (1), 100 (2), 200 (3) and 300 (4) atm (active gas present at trace level).

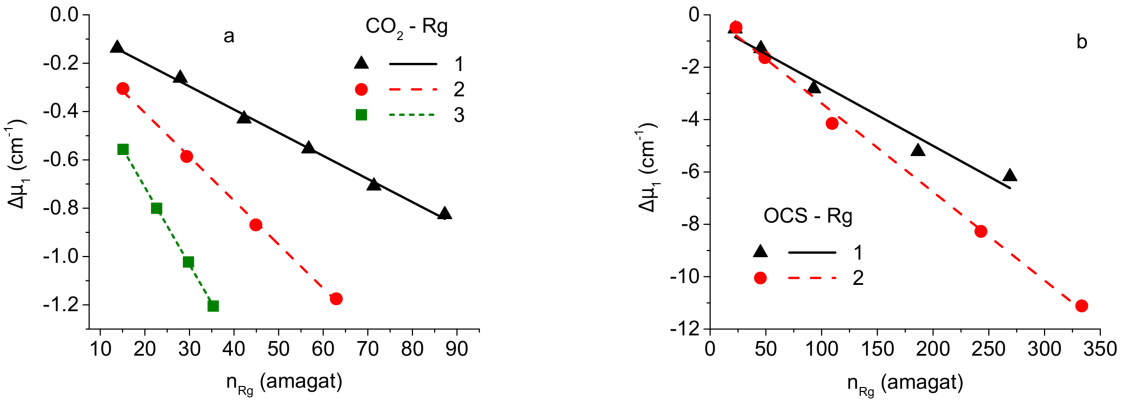

Figure 2: Deviations of the first moment $\Delta\mu_1 = \mu_1 - \mu_1^0$ with increasing gas density and corresponding linear fits for the ν_3 CO_2 (a) and $2\nu_3$ OCS (b) bands: perturbation by Ar (1), Kr (2) and Xe (3).

pressure, two cells were used: from 400 to 1000 cm^{-1} and pressures up to 100 atm a 13.5 cm cell with thallium bromoiodide (KRS-5) windows and from 1000 to 4500 cm^{-1} and pressures up to 300 atm a 7.4 cm cell with fluorite (CaF_2) windows. The mixtures were composed by pumping the compounds into a cell. The purity was controlled spectroscopically (no inpurity-gas bands were detected above the noise level).

Figure 1 shows examples of OCS band-shape transformation with increasing buffer-gas pressure. For both active molecules, the band origin was tracked by the first moment definition (numerical integration of Eq. (2) of Sec. 3.2 with the subsequent normalization). Examples of experimental band-origin shifts versus gas density and their linear fits can be seen in Fig. 2. The experimental band-origin shift coefficients are given in Tables 1 and 2.

Table 1: Spectral ν_3 band-origin shift coefficients γ (in 10^{-3} cm^{-1} amagat^{-1}) measured and calculated by the direct (Eq. (5)) and DID (Eq. (6)) methods for CO_2 perturbed by various rare gases. The references indicate the PES used for computations.

	expt	direct	DID
CO_2-Ar	-9.6(2)	-2.06 [16]	-6.28 [16], -6.57 [17], -6.27 [18]
CO_2-Kr	-18.2(2)	-9.51 [19]	-8.96 [19]
CO_2-Xe	-32.0(9)	-10.20 [20]	-13.29 [20], -2.83 [21], -3.36 [22]

Table 2: Experimental and DID-computed spectral band-origin shift coefficients γ (in 10^{-3} cm^{-1}amagat^{-1}) for various bands of OCS perturbed by Ar (PES [23]) and Kr (PES [24]).

	ν_3 band		$2\nu_3$ band		ν_2 band	
	expt	DID	expt	DID	expt	DID
OCS-Ar	-8(2)	-7.25	-23(2)	-14.50	-2(2)	-0.12
OCS-Kr	-19(2)	-11.32	-34(1)	-22.63	-5(2)	-0.18

3. Theory

3.1. Absorption coefficient and correlation function

An incident electromagnetic wave with angular frequency ω and intensity I_0, having propagated over a path length l in a media containing n_a absorbers per unit volume, looses its intensity I according to the Beer-Lambert law:

$$I(\omega) = I_0(\omega)e^{-n_a K(\omega)l}.$$

The absorption coefficient $K(\omega)$ is expressed [25] as

$$K(\omega) = \frac{4\pi^2\omega}{3\hbar c}\left(1 - e^{-\frac{\hbar\omega}{k_B T}}\right) F(\omega),$$

where $\hbar$, c and k_B stand for the Plank constant, speed of the electromagnetic wave in vacuum and Boltzmann constant, respectively, T is the temperature in Kelvin and $F(\omega)$ is the so-called spectral function. $F(\omega)$ may be regarded as the Fourier transform of a time correlation function $C(t)$ [26]:

$$F(\omega) = \frac{1}{2\pi}\int_{-\infty}^{\infty} dt e^{-i\omega t} C(t),$$

which is related to the dipole-moment absorption as

$$C(t) = \langle \mathbf{d}^\dagger(0)\mathbf{d}(t)\rangle. \quad (1)$$

Here, the dagger denotes the Hermitian conjugation and $\mathbf{d} = |v_f\rangle\langle v_f|\mathbf{D}|v_i\rangle\langle v_i|$ with $\langle v_f|\mathbf{D}|v_i\rangle$ standing for the vibrational $f \leftarrow i$ transition moment of the active-molecule dipole $\mathbf{D}$. The function $C(t)$, when known, determines completely $F(\omega)$ and, consequently, the full absorption band. To characterize the band-origin position we employ the spectral moments approach.

3.2. Spectral moments

The spectral moment of order n is defined by

$$M_n = \int_{-\infty}^{\infty} F(\omega)\omega^n d\omega. \tag{2}$$

Due to the fact that M_0 represents simply the integral intensity of the spectral band, normalized spectral moments $\mu_n = M_n/M_0$ are frequently used. From the Fourier-transform relationship $C(t) = \int_{-\infty}^{\infty} d\omega e^{i\omega t} F(\omega)$ one easily gets

$$\left.\frac{d^n C(t)}{dt^n}\right|_{t=0} = (i)^n \int_{-\infty}^{\infty} F(\omega)\omega^n d\omega.$$

Substitution of this equation in Eq. (2) gives

$$M_n = (-i)^n \left.\frac{d^n C(t)}{dt^n}\right|_{t=0}.$$

For our purposes the key interest is in the first spectral moment giving the band origin:

$$M_1 = -i \left.\frac{dC(t)}{dt}\right|_{t=0}.$$

With the definition (1) of $C(t)$ the time derivative can be re-written as

$$\left.\frac{dC(t)}{dt}\right|_{t=0} = \left.\left\langle \mathbf{d}^\dagger(0)\frac{d}{dt}\mathbf{d}(t)\right\rangle\right|_{t=0},$$

where

$$\frac{d}{dt}\mathbf{d}(t) = \frac{i}{\hbar}\left[H, \mathbf{d}(t)\right]$$

is determined by the commutator containing the full Hamiltonian H of the interacting molecule. The first spectral moment becomes

$$M_1 = \left\langle \mathbf{d}^\dagger(0)\left[H, \mathbf{d}(t)\right]\right\rangle/\hbar. \tag{3}$$

Moreover, H can be decomposed as a sum of the free-active-molecule Hamiltonian H_a and the absorber-perturber interaction term (PES) W:

$$H = H_a(\Omega, \mathrm{q}) + W(\mathbf{R}, \Omega, \mathrm{q}).$$

Here $\mathbf{R}$ is the intermolecular distance vector (between the centers of mass of the absorber and perturber), Ω specifies the active-molecule axis orientation and q is a set of vibrational coordinates. Thus, the rhs side of Eq. (3) reads

$$\left\langle \mathbf{d}^\dagger(0)\left[H, \mathbf{d}(t)\right]\right\rangle/\hbar = \left\langle \mathbf{d}^\dagger(0)\left[H_a, \mathbf{d}(t)\right]\right\rangle/\hbar + \left\langle \mathbf{d}^\dagger(0)\left[W, \mathbf{d}(t)\right]\right\rangle/\hbar.$$

The intermolecular potential W, in its turn, consists of the isotropic part $W^{iso}(R)$ and two compounds related to rotations and vibrations:

$$W(\mathbf{R}, \Omega, \mathrm{q}) = W^{iso}(R) + W^{rot}(\mathbf{R}, \Omega) + W^{vib}(\mathbf{R}, \Omega, \mathrm{q}).$$

The rotational perturbations W^{rot} and W^{iso} commute with the dipole moment $\mathbf{d}$ of a vibrational transition, thus the presence of solely rotational perturbation doesn't influence the value of the first spectral moment. For the vibrational transition $f \leftarrow i$ one gets

$$M_1 = M_0\mu_1^0 + M_0\langle W_{ff}^{vib} - W_{ii}^{vib}\rangle/\hbar \tag{4}$$

with the normalized first spectral moment in the absence of vibrational perturbation $\mu_1^0 = \langle v_f|H_a|v_f\rangle - \langle v_i|H_a|v_i\rangle$ and the double indices $ii(ff)$ denoting the vibrational diagonal matrix elements of $W^{vib}(\mathbf{R}, \Omega, \mathrm{q})$. Dividing Eq. (4) by M_0 one obtains

$$\mu_1 = \mu_1^0 + \gamma n_{Rg},$$

where n_{Rg} is the number density of the perturbing gas and the band-origin shift coefficient $\gamma = \langle W_{ff}^{vib} - W_{ii}^{vib}\rangle/(n_{Rg}\hbar)$ is introduced.

4. Band-origin shift computations

4.1. Direct computation of band shifts

Since the binary collision regime is confirmed by the linear dependence of measurements on n_{Rg} (see Fig. 2), the average required for the shifting coefficient calculation can be performed with the pair distribution function [27]:

$$\langle W_{ff}^{vib} - W_{ii}^{vib}\rangle = n_{Rg}\int d\mathbf{R}\int d\Omega e^{-\frac{W_{ii}}{k_BT}}(W_{ff}^{vib} - W_{ii}^{vib}), \tag{5}$$

where the first integral is a volume integral and the second one is the integral over the active molecule orientation; the diagonal matrix element W_{ii} corresponds to the full potential. Practical computations with Eq. (5) are determined by the availability of PES with vibrational dependence in the initial (typically, ground) and final (excited) states. Owing to relative simplicity of "linear molecule + atom" systems, their *ab initio* potential energy surfaces have been intensively studied in the literature. In the pioneering works, the absorbing molecule was treated as a rigid rotor [17, 18, 21, 22, 23, 24, 28], thus the vibrational dependence was totally neglected. However, accounting for antisymmetric stretching vibrations is essential for calculating band shifts [29] for both CO_2 and OCS. For direct computations we employed therefore only the vibrationally dependent potentials [16, 19, 20] constructed with noniterative inclusion of connected triples (CCSD(T)) and basis functions sets depending on the considered system.

4.2. Computation via dipole-induced dipole interaction

In the cases where vibrationally dependent PES are unavailable and Eq. (5) can not be used, evaluation of γ can be made with a simple model suggested bellow. Collisions with a polar active molecule may alter the spherical symmetry of the atomic perturber and induce on it an instantaneous dipole moment which will interact with the permanent (or transient) dipole of the molecule. This interaction can be a cause of the band origin shift. Indeed, the dipole moment $\mathbf{D}^{ind}$ induced on an atom placed in the electric field $\mathbf{E}$ is proportional to the atom polarizability α_{Rg}:

$$\mathbf{D}^{ind} = \alpha_{Rg}\mathbf{E},$$

and its potential energy reads

$$W^{ind} = -\frac{1}{2}\frac{\alpha_{Rg}}{R^6}(3\cos^2\theta + 1)D^2$$

with the angle between $\mathbf{D}$ and $\mathbf{R}$ denoted by θ. For a transition from the ground state i to a state f Eq. (5) becomes

$$\gamma = \frac{\pi\alpha_{Rg}}{\hbar}(\langle v_f|D^2|v_f\rangle - \langle v_i|D^2|v_i\rangle)\int_0^\infty \frac{dR}{R^4}\int_{-\pi/2}^{\pi/2} e^{-\frac{W_{ii}}{kT}}(3\cos^2\theta + 1)\sin\theta d\theta. \qquad (6)$$

In the harmonic approximation (D is proportional to q) one gets $\langle 1|D^2|1\rangle - \langle 0|D^2|0\rangle = \langle 2|D|1\rangle^2 = 2\langle 1|D|0\rangle^2$ and $\langle 2|D^2|2\rangle - \langle 0|D^2|0\rangle = 4\langle 1|D|0\rangle^2$. For our calculations, the transition dipole moments $d = \langle 1|D|0\rangle$ were taken as 0.374 D and 0.0473 D for the ν_3 and ν_2 OCS bands, [30] respectively, whereas $d = 0.3212$ D was used for the ν_3 band of CO_2 [31]. The polarizabilities α_{Rg} were 1.6404 [32], 2.4844 [33], 4.044 [34] Å^3 for Ar, Kr and Xe, respectively. The results of computations are presented in Tables 1 and 2.

5. Discussion

The bulk of our experimental and theoretical results is collected in Tables 1 (for CO_2) and 2 (for OCS). From the experimental standpoint, the band-origin shift coefficients appear to grow with increasing polarizability of the perturbing gas. Moreover, for the OCS case, the order of magnitude for the band shift for the ν_2 band is significantly smaller in comparison with that for the ν_3 band, which confirms the proportionality of the band shift to the dipole matrix element associated with the transition. Our experimental γ-value for CO_2-Ar ($(-8.9 \pm 0.2) \times 10^{-3}$ cm^{-1} amagat^{-1}) has the same order of magnitude as the datum published by Ozanne *et al.* [15] ($\gamma(\nu_3) = (-5.4 \pm 1.0) \times 10^{-3}$ cm^{-1} amagat^{-1}) and, likely their results for the ν_3 and $3\nu_3$ bands of CO_2-Ar, we find roughly the factor two between our measurements for ν_3 and $2\nu_3$ bands of OCS-Ar and OCS-Kr.

Due to the absence of vibrationally dependent potentials for OCS-Rg, direct calculations with Eq. (5) were feasible solely for CO_2-Rg cases, and comparison with the DID model (Eq. (5)) can be made for this absorbing molecule only (Table 1). In the case where the

same PES is used, for CO_2-Kr both methods give close results, but for CO_2-Ar and CO_2-Xe direct computation leads to a smaller absolute value of the band shift than the DID model. It can be noted also that the DID results for CO_2-Ar are very similar for various PES tested, while for CO_2-Xe choice of the potential plays a significant role.

To summarize, both computational methods may be reliably applied to CO_2/OCS mixtures with Ar, but with increase of the perturber polarisability the experiment gives significantly larger values. The nature of this discrepancy currently remains unclear and deserves further detailed consideration.

Acknowledgments

The authors are grateful for the financial support of the Russian Foundation of Fundamental Research (grant No. 19-03-00830). The spectra were recorded with core facilities of the "Geomodel" research center of St. Petersburg State University.

References

[1] Gordon RG. Molecular Motion and the Moment Analysis of Molecular Spectra. III. Infrared Spectra. J Chem Phys 1963;41(6):1819–29. doi:10.1063/1.1726162.

[2] Franz HB, Trainer MG, Malespin CA, Mahaffy PR, Atreya SK, Becker RH, et al. Initial SAM calibration gas experiments on Mars: Quadrupole mass spectrometer results and implications. Planet Space Sci 2017;138:44–54. doi:10.1016/j.pss.2017.01.014.

[3] Basilevsky A, Head J. The Surfaces of Venus. Rep Prog Phys 2003;66:1699–734. doi:10.1088/0034-4885/66/10/R04.

[4] Horn D, McAfee JM, Winer AM, Herr KC, Pimentel GC. The composition of the Martian atmosphere: Minor constituents. Icarus 1972;16(3):543–56. doi:10.1016/0019-1035(72)90101-7.

[5] Arney G, Meadows V, Crisp D, Schmidt SJ, Bailey J, Robinson T. Spatially resolved measurements of H_2O, HCl, CO, OCS, SO_2, cloud opacity, and acid concentration in the Venus near-infrared spectral windows. J Geophys Res: Planets 2014;119(8):1860–91. doi:10.1002/2014JE004662.

[6] Russo ND, DiSanti MA, Mumma MJ, Magee-Sauer K, Rettig TW. Carbonyl Sulfide in Comets C/1996 B2 (Hyakutake) and C/1995 O1 (Hale–Bopp): Evidence for an Extended Source in Hale–Bopp. Icarus 1998;135(2):377–88. doi:10.1006/icar.1998.5990.

[7] Moretto M, Feaga L, A'Hearn M. Abundances and spatial distributions of H_2O and CO_2 at comet 9P/Tempel 1 during a natural outburst. Icarus 2017;296:28–38. doi:10.1016/j.icarus.2017.05.013.

[8] Matthews H, MacLeod J, Broten N, Madden S, Friberg P. Observations of OCS and a search for OC_3S in the interstellar medium. Astrophys J 1987;315(2):646–53. doi:10.1086/165166.

[9] Minissale M, Congiu E, Manicò G, Pirronello V, Dulieu F. CO_2 formation on interstellar dust grains: A detailed study of the barrier of the CO+O channel. Astron Astrophys 2013;559:A49. doi:10.1051/0004-6361/201321453.

[10] Bouanich JP, Campers C, Blanquet G, Walrand J. Diode-laser measurements of Ar- and CO_2-broadened linewidths in the ν_1 band of OCS. JQSRT 1988;39(5):353–65. doi:10.1016/0022-4073(88)90100-8.

[11] Blanquet G, Walrand J, Bouanich JP, Boulet C. Line-mixing effects in Ar-broadened doublets of a hot band of OCS. J Chem Phys 1990;93(10):6962–70. doi:10.1063/1.459682.

[12] Domenech J, Bermejo D, Bouanich JP. Pressure Lineshift and Broadening Coefficients in the 2v3 Band of $^{16}O^{12}C^{32}$. J Mol Spectrosc 2000;200(2):266–76. doi:10.1006/jmsp.1999.8055.

[13] Thibault F, Boissoles J, Le Doucen R, Bouanich JP, Arcas P, Boulet C. Pressure induced shifts of CO_2 lines: Measurements in the 0003–0000 band and theoretical analysis. J Chem Phys 1992;96(7):4945–53. doi:10.1063/1.462737.

[14] Benner D, Miller C, Devi V. Constrained multispectrum analysis of CO_2-Ar broadening at 6227 and 6348 cm^{-1}. Can J Phys 2009;87(5):499–515. doi:10.1139/P09-014.
[15] Ozanne L, Ma Q, Nguyen-Van-Thanh, Brodbeck C, Bouanich J, Hartmann J,et al. Line-mixing, finite duration of collision, vibrational shift, and non-linear density effects in the ν_3 and $3\nu_3$ bands of CO_2 perturbed by Ar up to 1000 bar. JQSRT 1997;58(2):261–77. doi:10.1016/S0022-4073(97)00007-1.
[16] Cui Y, Ran H, Xie D. A new potential energy surface and predicted infrared spectra of the Ar- CO_2 van der Waals complex. J Chem Phys 2009;130(22):224311. doi:10.1063/1.3152990.
[17] Parker G, Snow R, Pack R. Intermolecular potential surfaces from electron gas methods. I. Angle and distance dependence of the He-CO_2 and Ar-CO_2 interactions. J Chem Phys 1976;64(4):1668–78. doi:10.1063/1.432340.
[18] Preston R, Pack R. Classical trajectory studies of rotational transitions in Ar-CO_2 collisions. J Chem Phys 1976;66(6):2480–87.
[19] Chen R, Zhu H, Xie D. Intermolecular potential energy surface, microwave and infrared spectra of the Kr-CO_2 complex from ab initio calculations. Chem Phys Lett 2011;511(4-6):229–34. doi: 10.1016/j.cplett.2011.06.067.
[20] Chen M, Zhu H. Potential energy surface, microwave and infrared spectra of the Xe-CO_2 complex from ab initio calculations. J Theor Comput Chem 2012;11(3):537–46. doi:10.1142/S0219633612500332.
[21] De Dios A, Jameson C. The ^{129}Xe nuclear shielding surfaces for Xe interacting with linear molecules CO_2, N_2, and CO. J Chem Phys 1997;107(11):4253–70. doi:10.1063/1.474800.
[22] Buck U, Huisken F, Otten D, Schinke R. Observation of multiple-collision rotational rainbows in Xe-CO_2: Comparison between TOF measurements and scattering calculations. Chem Phys Lett 1983; 101(2):126–30. doi:10.1016/0009-2614(83)87355-2.
[23] Zhu H, Guo Y, Xue Y, Xie D. Ab initio potential energy surface and predicted microwave spectra for Ar - OCS dimer and structures of Arn - OCS (n = 2-14) clusters. J Comput Chem 2006;27(9):1045–53. doi:10.1002/jcc.20421.
[24] Sun C, Shao X, Yu C, Feng E, Huang W. A three-dimensional potential energy surface and infrared spectra for the Kr-OCS van der Waals complex. Chem Phys Lett 2012;549:12–6. doi: 10.1016/j.cplett.2012.08.052.
[25] Hartmann JM, Boulet C, Robert D. Collisional effects on molecular spectra. Amsterdam: Elsevier; 2008.
[26] Gordon RG. Correlation Functions for Molecular Motion. Adv Magn Res 1968;3:1–42.
[27] Frommhold L. Collision Induced Absorption in Gases. Cambridge Monographs on Atomic, Molecular, and Chemical Physics. Cambridge: Cambridge University Press; 2006.
[28] Harris S, Janda K, Novick S, Klemperer W. Intermolecular potential between an atom and a linear molecule: The structure of ArOCS. Mol Phys 1975;63(2):881–4. doi:10.1063/1.431368.
[29] Chałasiński G, Szcześniak MM. State of the Art and Challenges of the ab Initio Theory of Intermolecular Interactions. Chem Rev 2000;100(11):4227–52. doi:10.1021/cr990048z. PMID: 11749345.
[30] Tanaka K, Tanaka T, Suzuki I. Dipole moment function of carbonyl sulfide from analysis of precise dipole moments and infrared intensities. J Comp Phys 1985;82(7):2835–44. doi:10.1063/1.448285.
[31] Johns J. Absolute intensities in CO_2: The 4.3- and 2.7-μm regions revisited. J Mol Spectrosc 1989; 134(2):433–9. doi:10.1016/0022-2852(89)90328-7.
[32] Hohm U, Kerl K. Interferometric measurements of the dipole polarizability a of molecules between 300K and 1100K II. A new method for measuring the dispersion of the polarizability and its application to Ar, H_2, and O_2. Mol Phys 1990;69(5):819–31. doi:10.1080/00268979000100621.
[33] Lide D.R. CRC Handbook of Chemistry and Physics, 85th Ed. Taylor & Francis, 2004.
[34] Teachout RR, Pack RT. The static dipole polarizabilities of all the neutral atoms in their ground states. At Data Nucl Data Tables 1971;3:195–214. doi:10.1016/S0092-640X(71)80007-4.